STUDY OF THE IMPEDANCE-RELATED INSTABILITIES IN THE FCC-ee DAMPING RING*

S. Bilanishvili†[1], A. De Santis[1], M. Migliorati[2,3], C. Milardi[1], M. Zobov[1]
[1]INFN Laboratori Nazionali di Frascati, Frascati, Italy
[2]Sapienza University of Rome, Rome, Italy
[3]INFN Sezione di Roma 1, Rome, Italy

Abstract

The design of the Future Circular Collider-ee damping ring is progressing, with ongoing optimisation of beam parameters and key accelerator systems. Accordingly, the coupling impedance model is updated to reflect the latest vacuum chamber and hardware layouts. In parallel, the estimates of collective effects and impedance-related instabilities are being refined. This paper presents the current wakefield and impedance models for the FCC-ee damping ring and reports the results of the respective instability studies, including possible mitigation strategies.

INTRODUCTION

The Future Circular Collider (FCC) is an ambitious project proposed at CERN to host, in a common tunnel, both a hadron collider (FCC-hh) and an electron–positron collider (FCC-ee) [1, 2]. The FCC-ee is foreseen to operate at four main energy stages, corresponding to the Z, W, Higgs, and top-quark pair production regimes [3]. These operation modes require high beam quality and therefore place demanding requirements on the injector complex.

The FCC-ee injector complex includes a damping ring designed to reduce the transverse emittance before beam injection into the collider [4]. Since the damping-ring design is still evolving, the beam and machine parameters used in this study are those presented at FCC Week 2025 and are summarised in Table 1 [5]. This parameter set corresponds to a 2.86 GeV ring with a circumference of about 373 m, a natural bunch length of approximately 5 mm, and up to 40 stored bunches. The parameters listed in Table 1 define the reference working point used for the present beam-stability studies. In particular, they are used to evaluate the impact of wakefields and coupling impedance on single-bunch and multi-bunch collective effects [6, 7]. The impedance model of the FCC-ee damping ring is being developed together with the optimisation of the vacuum chamber and accelerator hardware. Contributions from the resistive wall and from selected vacuum chamber components are included in order to estimate their impact on the beam dynamics. In the following paragraphs the current status of the wakefield model for the FCC-ee damping ring is presented and the corresponding impedance related instabilities are analyzed.

* This work was done in the framework of the ADDENDUM FCC-GOV-CC0205(KE 4907), between INFN-LNF and CERN.
† shalva.bilanishvili@lnf.infn.it

Table 1: FCC-ee damping ring parameters used in the simulations.

Parameter	Value
Energy [GeV]	2.86
Circumference [m]	373.46
Natural emittance [nm rad] (WGL on/off)	1.3 / 2.3
Bunch length [mm]	5.1
Damping time $\tau_{x,y}$ [ms] (WGL on/off)	16.9 / 29.4
Natural chromaticity (x/y)	$-38.2/-28.3$
Natural energy spread (WGL on/off) [10^{-4}]	7.1 / 5.2
Betatron amplitude max. (x/y) [m]	9.66 / 6.49
Betatron amplitude min. (x/y) [m]	0.5 / 1.1
Tune (Q_x, Q_y)	27.8707 / 22.3728
Momentum compaction (WGL on/off) [10^{-3}]	1.55 / 1.57
Revolution period [μs]	1.2457
Max. number of stored bunches / bunch current [mA]	40 / 4
Energy loss per turn (WGL on/off) [keV]	422.2 / 246.7
SR power loss in wigglers [kW]	27.83
Bunch population, N_{part}	$3.120\,75 \times 10^{10}$
Bunch current, I_{bunch} [A]	0.003 964 02

IMPEDANCE MODEL

The impedance model of the FCC-ee damping ring includes the resistive wall of the vacuum chamber and a first set of representative vacuum hardware components. Since the damping-ring layout is still evolving, the model is based on preliminary geometries and component counts estimated from modern storage-ring examples. In particular, the number of BPMs, bellows, flange joints and vacuum transitions was evaluated by comparison with several reference machines [8–15]. The studied component designs follow low-impedance concepts already used or proposed in existing storage rings and can be adapted to the FCC-ee damping-ring vacuum system.

The longitudinal and transverse wake potentials for a 5 mm Gaussian bunch, obtained from electromagnetic simulations with CST Studio Suite, are shown in Figs. 1 and 2, respectively [16]. These wake potentials are used to compare the relative importance of the different impedance sources and to define a preliminary impedance budget.

The resistive-wall contribution was evaluated with IW2D for stainless-steel vacuum chambers coated with a 100 nm NEG layer [17–21]. This material choice is motivated by electron-cloud studies for FCC-ee damping-ring vacuum-chamber options, where NEG-coated chambers were con-

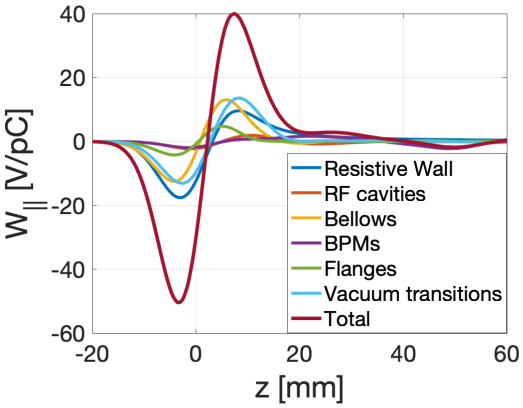

Figure 1: Longitudinal wake potentials of a 5 mm Gaussian bunch.

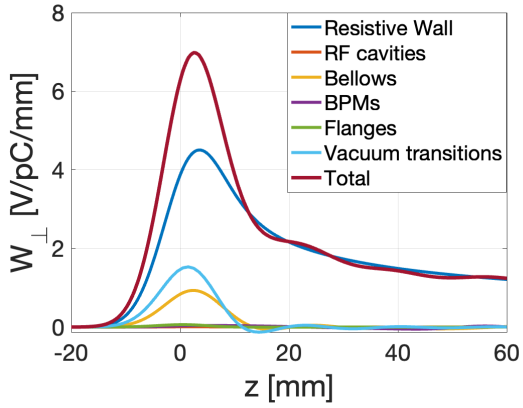

Figure 2: Transverse wake potentials of a 5 mm Gaussian bunch.

sidered for electron-cloud mitigation [22]. Stainless steel is used as a conservative choice, while the NEG coating is relevant for vacuum performance and for reducing the effective secondary electron yield. Three aperture regions were considered: a 30 mm radius for the straight sections, a 15 mm radius for the arc regions, and a 5 mm half-gap for the wiggler sections. The corresponding lengths were assigned according to the damping-ring parameter set used in this study. Several representative vacuum components were also simulated. The bellows model is based on an RF-shielded structure with omega-shaped strips, inspired by the DAΦNE design, and was simulated for a 30 mm beam-pipe radius. A button BPM geometry with 6 mm radius buttons, a 1 mm gap, and dielectric constant $\varepsilon_r = 4.5$ was included for the same aperture. The RF cavity contribution was estimated using a 400 MHz superconducting cavity geometry developed for the FCC-ee collider rings [23]. Flange-joint and vacuum-transition models were also simulated for a 30 mm vacuum-chamber radius; in the flange model, the spring-seal structure produces a 1×2 mm gap between adjacent vacuum-chamber walls. The loss and kick factors obtained from the 5 mm wake-potential calculations are listed in Table 2. The values are multiplied by the corresponding number of components considered in the present damping-ring model. They therefore represent the estimated contribution of each component family to the preliminary impedance budget, rather than the contribution of a single element.

Table 2: Loss and kick factors for the considered damping-ring impedance contributions. The values are multiplied by the corresponding number of devices.

Component	Loss [V/pC]	Kick [V/pC/mm]
RW full machine	7.101 139	3.220 681
RF cavities	$2.654\,752 \times 10^{-4}$	$5.648\,135 \times 10^{-3}$
Button BPMs	1.084 894 4	0.026 804 64
Bellows	1.063 910 75	0.630 745 15
Flanges	0.028 383 5	0.041 502 0
Vac. transitions	3.956 34	1.044 267

Short-bunch wakefields corresponding to a 0.4 mm Gaussian bunch were also calculated and used as pseudo-Green functions for tracking studies, [24, 25]. For the azimuthally symmetric structures, such as RF cavity, vacuum transitions and flanges, the 0.4 mm pseudo-Green-function wakes were evaluated with ECHO2D [26], while the resistive-wall contribution was obtained with IW2D [17]. The present single-bunch instability studies are therefore based on this reduced short-bunch wake set.

LONGITUDINAL EFFECTS

Longitudinal tracking simulations were performed with Xsuite to evaluate the bunch length and energy spread as a function of bunch population [27]. The FCC-ee damping-ring parameter set considered here has a natural bunch length of about 5.1 mm and a momentum compaction factor of $\alpha_c \simeq 1.55 \times 10^{-3}$. Together with the relatively large vacuum aperture required to accept the injected positron beam before damping, these parameters are expected to increase microwave-instability threshold.

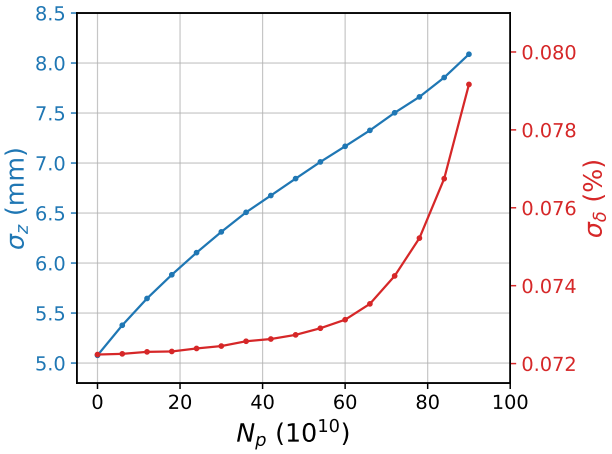

Figure 3: Bunch length and relative energy spread as a function of bunch population. Note that the nominal bunch intensity is 3.12e10.

The simulation results are shown in Fig. 3. For the impedance model considered so far, the nominal bunch

population is well below the microwave-instability threshold [28–30]. Around nominal intensity range, the bunch lengthening is interpreted as potential-well distortion, since no significant energy-spread growth is observed. At higher bunch population, close to the instability threshold, the longitudinal phase-space distribution becomes distorted and the energy spread starts to increase. The longitudinal phase space just below, on the edge, and above the microwave-instability threshold is shown in Fig. 4. The distribution is plotted in the (z, δ) plane, where $\delta = (p - p_0)/p_0$ is the relative momentum deviation. For the ultra-relativistic beam considered here, δ is practically equivalent to the relative energy deviation.

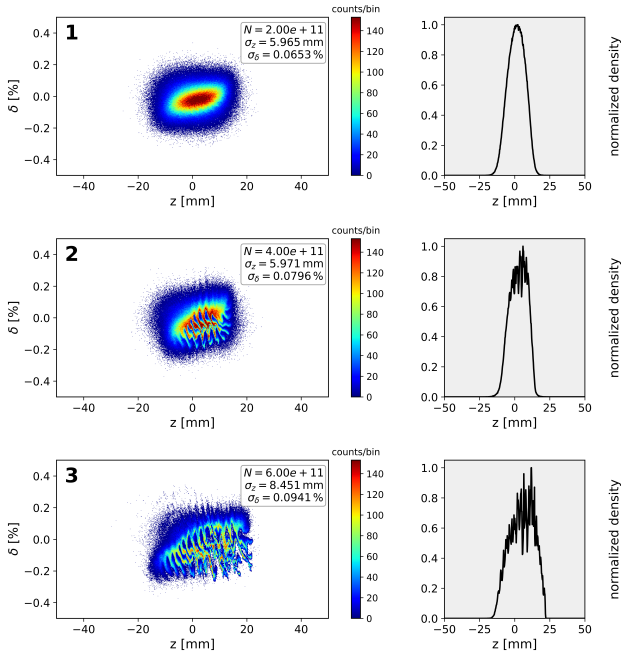

Figure 4: Longitudinal phase-space distributions for different bunch populations .

These results suggest that longitudinal single-bunch effects are not expected to be critical at the nominal bunch population for the present FCC-ee damping-ring impedance model.

TRANSVERSE EFFECTS

The transverse mode-coupling instability (TMCI) is one of the main single-bunch effects driven by transverse wakefields [31]. In this instability, the coherent transverse oscillation modes shift with bunch intensity and can merge, leading to unstable transverse motion. The threshold depends on the transverse wakefields, the synchrotron tune, and the longitudinal bunch distribution. The coherent mode spectra were obtained from the turn-by-turn evolution of the bunch moments for different bunch populations. Figure 5 shows the real part of the coherent tune shift, normalized to the zero-current synchrotron tune, as a function of bunch population.

For the considered impedance model, no TMCI threshold is observed close to the nominal bunch population. The lowest coherent modes remain separated over the intensity range relevant for nominal operation, and the instability threshold is found to be well above the nominal value. This result is consistent with the relatively long nominal bunch length and with the larger aperture required to accept the injected positron beam before damping. Additional contributions, in particular from BPMs and bellows, will be included in future simulations as the damping-ring impedance model is completed. In addition to the single-bunch TMCI, multi-bunch transverse instabilities can be driven by the low-frequency resistive-wall impedance [32, 33]. Therefore, first estimates of the coupled-bunch instability have been performed. At present, the need for a transverse feedback kicker is not yet clear, since the damping time has been reduced from about 16 ms to about 6 ms, which may already be sufficient to suppress the instability, [34].

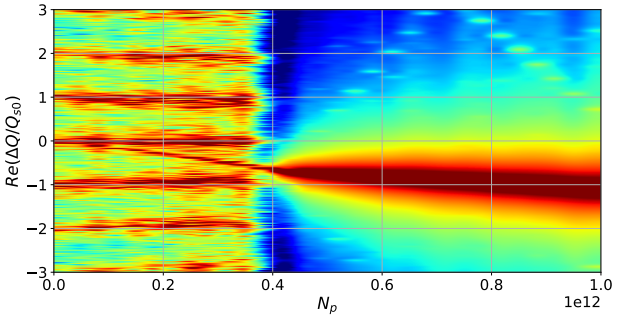

Figure 5: Coherent transverse mode spectrum as a function of bunch population. Note that the nominal bunch intensity is 3.12e10.

CONCLUSION

A preliminary impedance model for the FCC-ee damping ring has been assembled using resistive-wall calculations and wakefield simulations of representative vacuum chamber components. Wake potentials calculated for the nominal 5 mm bunch length were used to compare the relative importance of the different impedance sources and to estimate the corresponding loss and kick factors. The 0.4 mm short-bunch wake potentials were used as pseudo-Green functions for the presented single-bunch tracking studies. For the impedance model considered so far, the longitudinal simulations show no significant bunch lengthening or energy-spread growth at the nominal bunch population. The transverse simulations do not indicate a TMCI threshold close to the nominal bunch population.

REFERENCES

[1] A. Abada *et al.*, "FCC-hh: The Hadron Collider", *Eur. Phys. J. Spec. Top.*, vol. 228, pp. 755–1107, 2019. doi:10.1140/epjst/e2019-900087-0

[2] A. Abada *et al.*, "FCC-ee: The Lepton Collider", *Eur. Phys. J. Spec. Top.*, vol. 228, pp. 261–623, 2019. doi:10.1140/epjst/e2019-900045-4

[3] A. Abada *et al.*, "FCC physics opportunities", *Eur. Phys. J. C*, vol. 79, p. 474, 2019. doi:10.1140/epjc/s10052-019-6904-3

[4] O. Etisken *et al.*, "Considerations for a new damping ring design for the FCC-ee injector complex", in *Proc. IPAC'23*, Venice, Italy, May 2023, pp. 943–946. doi:10.18429/JACoW-IPAC2023-MOPL175

[5] A. De Santis *et al.*, "FCC-ee injector: New DR at 2.86 GeV", presented at FCC Week 2025, Vienna, Austria, May 2025.

[6] L. Palumbo, V. G. Vaccaro, and M. Zobov, "Wake fields and impedance", CERN Yellow Rep. CERN-95-06, pp. 331–390, 1995, e-Print: physics/0309023.

[7] K. Y. Ng, *Physics of Intensity Dependent Beam Instabilities*. Singapore: World Scientific, 2006.

[8] L. Ducimetière *et al.*, "Beam position monitor system for the ESRF Extremely Brilliant Source", in *Proc. IBIC'19*, Malmö, Sweden, Sep. 2019, pp. 1–6. doi:10.18429/JACoW-IBIC2019-MOA003

[9] J. M. Filhol *et al.*, "Design of the BPM system for the SOLEIL II storage ring", in *Proc. IBIC'24*, Beijing, China, Sep. 2024, paper TUP44.

[10] M. C. Charrondière *et al.*, "SLS 2.0 vacuum components design", in *Proc. IPAC'23*, Venice, Italy, May 2023, pp. 4266–4269. doi:10.18429/JACoW-IPAC2023-THPA147

[11] A. Blednykh, S. Krinsky, B. Podobedov, J. Rose, N. Towne, and J.-M. Wang, "Collective effects for NSLS-II", in *Proc. PAC'05*, Knoxville, TN, USA, May 2005, paper MPPP036.

[12] A. Blednykh *et al.*, "Impedance of the flange joints with the RF contact spring in NSLS-II", in *Proc. IPAC'19*, Melbourne, Australia, May 2019, pp. 1597–1600. doi:10.18429/JACoW-IPAC2019-TUPGW082

[13] E. Al-Dmour *et al.*, "The MAX IV 3 GeV storage ring vacuum system", *J. Synchrotron Radiat.*, vol. 28, pp. 712–718, 2021. doi:10.1107/S1600577521002426

[14] S. Tomassini *et al.*, "A new RF shielded bellows for DAΦNE upgrade", in *Proc. EPAC'08*, Genoa, Italy, Jun. 2008, pp. 1653–1655.

[15] F. Marcellini, M. Serio, A. Stella, and M. Zobov, "DAΦNE broad-band button electrodes", *Nucl. Instrum. Methods Phys. Res. A*, vol. 402, pp. 27–35, 1998. doi:10.1016/S0168-9002(97)01083-8

[16] Dassault Systèmes, *CST Studio Suite*. https://www.3ds.com/products/simulia/cst-studio-suite

[17] N. Mounet, "The LHC transverse coupled-bunch instability", Ph.D. thesis, EPFL, Lausanne, Switzerland, 2012.

[18] E. Belli, G. Castorina, M. Migliorati, A. Novokhatski, S. Persichelli, B. Spataro, and M. Zobov, "Coupling impedances and collective effects for FCC-ee", in *Proc. IPAC'17*, Copenhagen, Denmark, May 2017, pp. 3734–3737. doi:10.18429/JACoW-IPAC2017-THPAB020

[19] M. Migliorati, E. Belli, and M. Zobov, "Impact of the resistive wall impedance on beam dynamics in the Future Circular Collider", *Phys. Rev. Accel. Beams*, vol. 21, p. 041001, 2018. doi:10.1103/PhysRevAccelBeams.21.041001

[20] E. Belli *et al.*, "Electron cloud buildup and impedance effects on beam dynamics in the Future Circular e^+e^- Collider and experimental characterization of thin TiZrV vacuum chamber coatings", *Phys. Rev. Accel. Beams*, vol. 21, p. 111002, 2018. doi:10.1103/PhysRevAccelBeams.21.111002

[21] P. Chiggiato and R. Kersevan, "Synchrotron radiation-induced desorption from a NEG-coated vacuum chamber", *Vacuum*, vol. 60, pp. 67–72, 2001. doi:10.1016/S0042-207X(00)00247-5

[22] O. Etisken *et al.*, "Electron cloud studies for DAΦNE collider and e^+e^- future circular collider damping ring", *Nucl. Instrum. Methods Phys. Res. A*, vol. 1082, p. 171019, 2026. doi:10.1016/j.nima.2025.171019

[23] S. Gorgi Zadeh, "Accelerating cavity and higher order mode coupler design for the Future Circular Collider", Ph.D. thesis, University of Rostock, Rostock, Germany, 2021.

[24] K. L. F. Bane and M. Sands, "Wakefields of very short bunches in an accelerating cavity", *Part. Accel.*, vol. 25, pp. 73–95, 1990.

[25] A. W. Chao, *Physics of Collective Beam Instabilities in High Energy Accelerators*. New York, NY, USA: Wiley, 1993.

[26] I. Zagorodnov and T. Weiland, "TE/TM field solver for particle beam simulations without numerical Cherenkov radiation", *Phys. Rev. ST Accel. Beams*, vol. 8, p. 042001, 2005. doi:10.1103/PhysRevSTAB.8.042001

[27] G. Iadarola *et al.*, "Xsuite: An integrated beam physics simulation framework", in *Proc. HB'23*, Geneva, Switzerland, Oct. 2023, pp. 73–80. doi:10.18429/JACoW-HB2023-TUA2I1

[28] E. Keil and W. Schnell, "Concerning longitudinal stability in the ISR", CERN, Geneva, Switzerland, Rep. CERN-ISR-TH-RF/69-48, 1969.

[29] D. Boussard, "Observation of microwave longitudinal instabilities in the CPS", CERN, Geneva, Switzerland, Rep. CERN-LabII/RF/Int./75-2, 1975.

[30] F. J. Sacherer, "A longitudinal stability criterion for bunched beams", *IEEE Trans. Nucl. Sci.*, vol. 20, no. 3, pp. 825–829, 1973. doi:10.1109/TNS.1973.4327254

[31] F. J. Sacherer, "Transverse bunched beam instabilities: Theory", in *Proc. 9th Int. Conf. High Energy Accelerators*, Stanford, CA, USA, 1974, pp. 347–351.

[32] E. Métral, "Transverse resistive-wall impedance from very low to very high frequencies", CERN, Geneva, Switzerland, Rep. CERN-AB-2005-084, 2005.

[33] A. Blednykh, G. Bassi, C. Hetzel, B. Kosciuk, and V. Smaluk, "NSLS-II longitudinal impedance budget", *Nucl. Instrum. Methods Phys. Res. A*, vol. 1005, p. 165349, 2021. doi:10.1016/j.nima.2021.165349

[34] C. Milardi, "Damping ring for FCC-ee injector complex", presented at Joint WP3–WP4 meeting, Mar. 2026.